Journal of the Korean Nuclear Society
Volume 36, Number 1, pp.73~82, February, 2004

Fault Detection and Diagnosis of the Deaerator Level Control System in Nuclear Power Plants

Kyung Youn Kim and Yoon Joon Lee
Cheju National Unversity
Ara1-dong, Cheju City, 694-756, Korea
leeyj@cheju.ac.kr

(Received August 12, 2003)

Abstract

The deaerator of a power plant is one of feedwater heaters in the secondary system, and it is located above the feedwater pumps. The feedwater pumps take the water from the deaerator storage tank, and the net positive suction head(NSPH) should always be ensured. To secure the sufficient NPSH, the deaerator tank is equipped with the level control system of which level sensors are critical items. And it is necessary to ascertain the sensor state on-line. For this, a model-based fault detection and diagnosis(FDD) is introduced in this study. The dynamic control model is formulated from the relation of input-output flow rates and liquid-level of the deaerator storage tank. Then an adaptive state estimator is designed for the fault detection and diagnosis of sensors. The performance and effectiveness of the proposed FDD scheme are evaluated by applying the operation data of Yonggwang Units 3 & 4.

Key Words : deaerator, liquid-level control, fault detection and diagnosis, adaptive estimator

1. Introduction

Since the safety and reliability are critical issues in nuclear fields, the nuclear plants are usually provided with various hardware redundancies. And recently, the software redundancies for the measurement and control system such as fault detection and diagnosis have drawn a great attention as a complementary approach to increase the plant safety. The fault detection and diagnosis techniques have been employed in numerous fields of industry, and is becoming more important with the expansion of industrial automation.

The fault detection and diagnosis techniques developed so far could be classified into two categories, that is, a knowledge based technique and a model based technique[1-3]. The knowledge based technique does not need the physical model of a given system, but, instead, it requires constructing the database which describes all the potential faults of the system. On the other hand, the model based technique needs the system model, as its name implies. But in this model based technique, a database is not necessary and unexpected faults could be detected[4-6].

The model based fault detection and diagnosis technique is based on the analysis of the given system and is divided further into two methods of the parameter estimation and the state estimation. In the parameter estimation, the variation of the actual system parameters, obtained from the relations between estimated parameters and actual parameters, are used to identify the faults[7]. However, the non-linearity between the actual model parameters and the estimated parameters makes it difficult to define the relationship exactly[8]. Until now, various methods for the parameter estimation have been developed. For an example, the pattern recognition method obtains the parameter errors between the estimated model and the normal model and uses these errors to identify the faults[9], and even the neural circuits are exploited for the parameter estimation.

The state estimation includes many methods ranging from the parity check to the innovation verification by use of Kalman filter or observer, and to the error sensing filter[10]. All these methods use the errors between the measured output and the estimated output. Among numerous methods of state estimation, the multiple model method is known to be more efficient and flexible in identifying the faults than other methods[11-13].

The deaerator of a nuclear power plant is one of the heaters of the secondary system, and it is located above the feedwater pumps. The feedwater pumps take the water from the deaerator storage tank, and the net positive suction head(NPSH) should always be ensured. During the normal operation, the deaerator operates in the saturated state and maintains the designed operating NPSH. But it may experience significant pressure decay during two-phase transient situations and in the worst case, the cavitation may occur, resulting in a plant trip. To

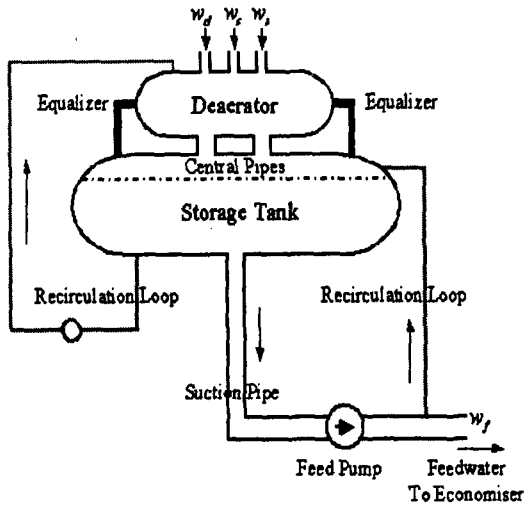

Fig. 1. Deaerator System

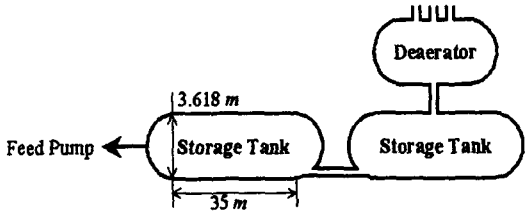

Fig. 2. Geometric Structure of the Deaerator System

secure the sufficient NPSH, the deaerator tank is equipped with the level control system of which level sensors are critical items, and it is important to ascertain the functional states of sensors.

In this paper, a fault detection and diagnosis system for the deaerator level control system is developed using the state estimation techniques based on multiple model. The geometrical structure of the deaerator storage tank and the input and output flow rates under the steady state are used to set up the dynamic control model which is described in terms of state equations and measurement equations. Then a fault detection and diagnosis method is developed making use of an adaptive estimator to check the integrity of

level measurement sensors. Finally, the proposed method is verified and evaluated by applying to Yonggwang Units 3 & 4.

2. Deaerator Model

The oxygen and other active gases dissolved in the secondary condensate water cause the corrosion of the system resulting in the plant life shortening. The deaerator, the fourth heater in case of Yonggwang, removes the dissolved gases from the condensate water and at the same time heats up the condensate water to increase the plant efficiency. The feedwater free of dissolved gases runs into the storage tank whose level is maintained within a predetermined range. Then the water is pumped out of the storage tank into the next heater. This is described in Fig. 1.

The deaerator has three inputs: condensate water w_c from condenser through the previous heater, extraction steam w_s from low pressure turbine, and drains w_d from the next heater. The central pipes link the deaerator and storage tank and equalizers are provided to balance the pressures of the two tanks. The suction pipe is used to establish a suction head for the feedwater pumps.

Figure 2 shows the geometrical structure of the deaerator in Yonggwang Units 3 & 4. The total volume of the two storage tanks is $746m^3$[14], while the cylindrical portions, excluding the hemispheric parts, of the tanks is found to be $720m^3$. The difference is the volume of four dishes at the ends of each tank. To make the problem simple, the actual two hemisherical tanks are replaced with one cylindrical tank with the same volume of $746m^3$. Then the deaerator storage tank could be presented by a cylindrical tank whose dimension is 3.68m in diameter and 70m in length.

To establish the dynamic model which describes the relation between the storage tank level and

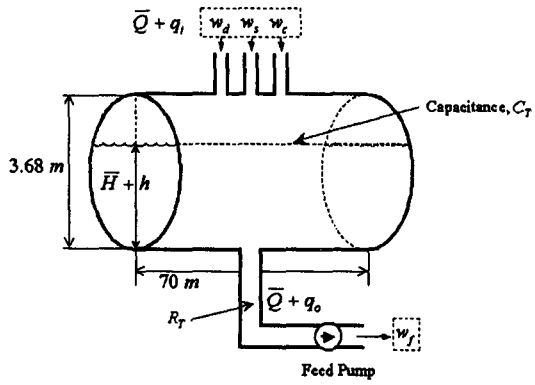

Fig. 3. Flow and Level of the Deaerator

flow rates, the analogy of electrical resistance and capacitance is introduced as shown in Fig. 3[15]. In this figure, $\overline{H}$ is the level in a steady state and h is the deviation from $\overline{H}$. And $\overline{Q}$, m^3/s, is the normal flow rate, and q_i and q_o denote flow rate deviations from steady inlet and outlet flow rates, respectively.

The variation of the condensate in storage tank during dt is

$$C_T dh = (q_i - q_o)\,dt \tag{1}$$

where C_T is the tank capacitance defined as

$$C_T = \frac{\text{variation of condensate volume , } m^3}{\text{variation of condensate head , } m} \tag{2}$$

Therefore, the tank capacitance is the surface area of the condensate as described in Fig. 3. The tank resistance at the outlet, R_T, is defined as

$$R_T = \frac{\text{variation of head, } m}{\text{variation of outlet flow rate, } m^3/s} \tag{3}$$

However, the head has relation to the flow rate in a non-linear manner. Figure 4 is the characteristic curve between the head and flow rate. The non-linearity shown in the figure is due to the circular vertical cross section of the tank. With the assumption that the variations are small, a linearity

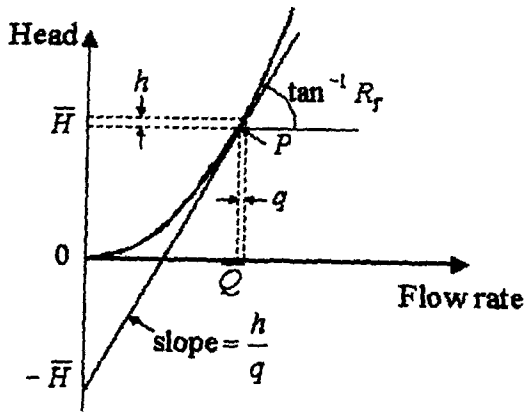

Fig. 4. Characteristic Curve between Head and Flow Rate

could be obtained around the steady state point P. Then the resistance at the outlet is

$$R_T = \frac{dH}{dQ} = \frac{dh}{q_o} \tag{4}$$

From Eqs. (1) and (4), the rate of change of the head is found to be

$$\frac{dh(t)}{dt} = -\frac{1}{R_T C_T} h(t) + \frac{1}{C_T} q_i(t) \tag{5}$$

3. Fault Detection and Diagnosis by an Adaptive Estimator

The adaptive estimator was developed by Moose[16] for the tracking of maneuvering target, and it has been proven to be efficient in estimating the position, velocity, acceleration and radar bias. The idea of this adaptive estimator is applied to the fault detection and diagnosis of deaerator level sensors.

3.1. Modeling of Dynamic System

The model described by Eq. (5) is cast into the stochastic discrete state equation of:

$$x_{k+1} = F x_k + G u_k + T w_k \tag{6}$$

where x_k = state vector at time k, u_k = input vector, F = state transition matrix, G = control input matrix, T = noise gain matrix, and w_k = white Gaussian process noise with the covariance of

$$E[w_k w_l^T] = \Gamma_w \delta_{kl}\ ,\ \delta_{kl} = \text{Kronecker delta} \tag{7}$$

On the other hand, the measurement equation with random measurement sensor bias is

$$z_k = H x_k + v_k + v^b \tag{8}$$

where z_k = measurement vector at time, k, H = measurement matrix, and v_k = white Gaussian measurement noise with the covariance of

$$E[v_k v_l^T] = \Gamma_v \delta_{kl} \tag{9}$$

Further, the process noise and measurement noise are assumed to be independent each other. Then

$$E[v_k w_l^T] = 0,\ \forall\ k \text{ and } l \tag{10}$$

In Eq. (8), v^b presents the bias vector, and is assumed to be governed by the semi-Morkov process. A semi-Morkov process is different from

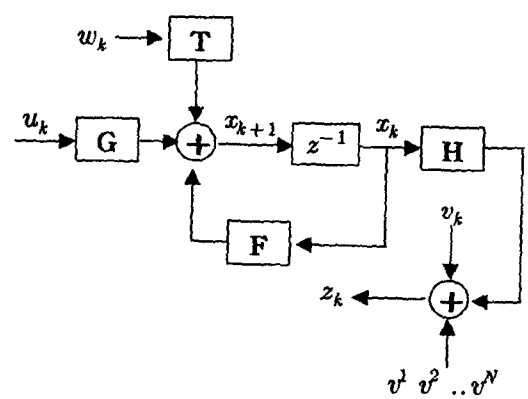

Fig. 5. Block Diagram of the Dynamic System with Biases

a Markov process in that the duration of time of one state before switching to another state is itself a random variable. The block diagram of the dynamic system model described so far is shown in Fig. 5.

3.2. Kalman Filter

If the measurement sensor does not include the bias v^b, it is possible to construct the Kalman filter in which a time updating step and a measurement updating step iterate. The time updating is the one step ahead prediction of

$$\hat{x}_{k|k-1} = F\hat{x}_{k-1|k-1} + Gu_{k-1} \tag{11}$$

$$P_{k|k-1} = F P_{k-1|k-1} F^T + T\Gamma_w T^T \tag{12}$$

And the measurement updating is accomplished by filtering of

$$K_k = P_{k|k-1} H^T (S_k)^{-1} \tag{13}$$

$$\hat{x}_{k|k} = \hat{x}_{k|k-1} + K_k e_k \tag{14}$$

$$P_{k|k} = (I - K_k H) P_{k|k-1} \tag{15}$$

where,

$$e_k = z_k - H\hat{x}_{k|k-1} \tag{16}$$

$$S_k = H P_{k|k-1} H^T + \Gamma_v \tag{17}$$

In above equations, $\hat{x}_{k|k}$ denotes the estimated state vector. K_k is a Kalman gain matrix, and $P_{k|k} = E[(x - \hat{x}_{k|k})(x - \hat{x}_{k|k})^T$ is the covariance matrix of system state errors.

3.3. Adaptive Estimator

If the measurement sensor include the bias v^b, an adaptive estimator could be established making use of the conditional probability theory of Bayes. The block diagram of the adaptive estimator which consists of a state estimation part and a bias estimation part is shown in Fig. 6. Ref. [16] reads the details on the derivation of each block, and summarized below are governing equations of each block.

3.3.1. *i-th* Kalman Filter

Time-updating step

$$\hat{x}^i_{k|k-1} = F\hat{x}^i_{k-1|k-1} + Gu_{k-1} \tag{18}$$

$$P^i_{k|k-1} = FP^i_{k-1|k-1} F^T + T\Gamma_w T^T \tag{19}$$

Measurement-updating step

$$K^i_k = P^i_{k|k-1} H^T (S^i_k)^{-1} \tag{20}$$

$$\hat{x}^i_{k|k} = \hat{x}^i_{k|k-1} + K^i_k e^i_k \tag{21}$$

$$P^i_{k|k} = (I - K^i_k H) P^i_{k|k-1} \tag{22}$$

where,

$$e^i_k = z_k - H\hat{x}^i_{k|k-1} - v^i \tag{23}$$

$$S^i_k = H P^i_{k|k-1} H^T + \Gamma_v + \Gamma^i_b \tag{24}$$

In these equations, S^i_k is the i-th residual covariance matrix, and e^i_k is the i-th residual vector.

Finally, $P^i_{k|k} = E[(x - \hat{x}^i_{k|k})(x - \hat{x}^i_{k|k})^T]$ is the covariance matrix of state error and $\Gamma^i_b = E[(v^b - v^i)(v^b - v^i)^T]$ is the covariance matrix of biases.

3.3.2. Calculation of Weights

The weighting matrix of each filter is

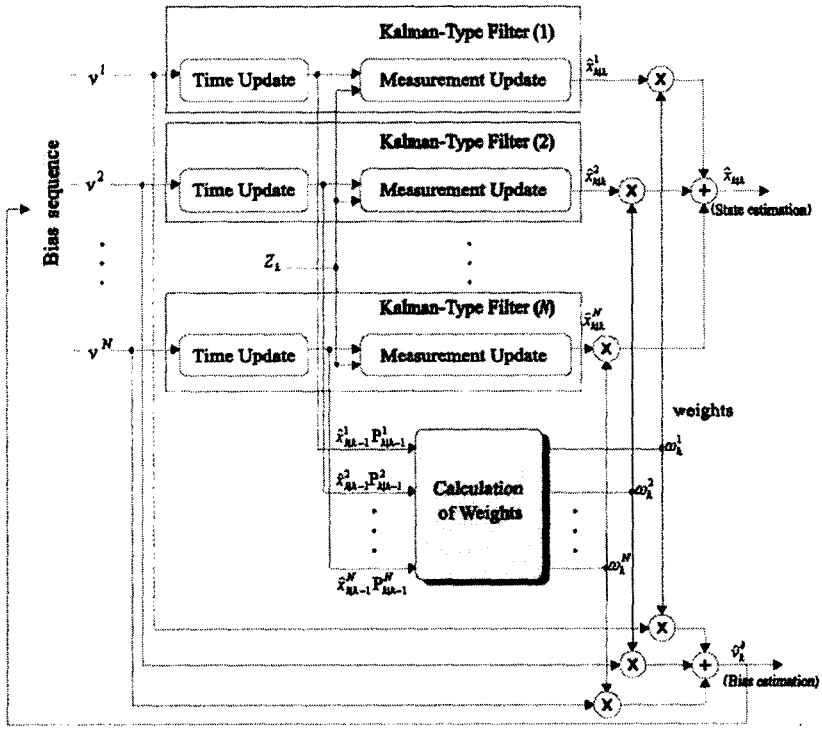

Fig. 6. Block Diagram of Adaptive Estimator

$$W_k = c_k L_k \Theta^T W_{k-1} \tag{25}$$

The i-th element of W_k is ω_k^i, and L_k is the diagonal matrix whose elements are

$$\rho_{ii} = \exp\left(-\frac{1}{2}(e_k^i)^T (S_k^i)^{-1}(e_k^i)\right) \tag{26}$$

Θ is the Markov transition matrix with the pre-determined elements of θ_{ij}, and c_k is determined to satisfy the following condition at every calculational iteration.

$$\sum_{i=1}^{N} \omega_k^i = 1 \tag{27}$$

3.3.3. State Estimation and Bias Estimation

The estimated states are obtained from

$$\hat{x}_{k|k} = \sum_{i=1}^{N} \hat{x}^{\,i}_{k|k} W_k \tag{28}$$

and the unknown sensor bias is estimated from the equation of

$$\hat{v}_k^b = V^T W_k \tag{29}$$

where V is the assumed bias vector of N elements.

4. Application and Evaluation

To evaluate the performance of identifying level sensor faults, actual operating data of Yonggwang Units 3 & 4 deaerator are applied to the proposed deaerator model for the level control and to the adaptive estimator. Figure 7 shows the inlet and outlet flow rates of the deaerator when the plant is in the steady state of full power.

As shown in the figure, the flow rate in a steady

state is $\overline{Q}$ = 1605.92*kg/sec*, and the normal level is 70% of the inner diameter of the storage tank, that is, $\overline{H}$ = 3.68m × 70‰ = 2.576*m*. The capacitance of the tank is determined as 236.1m^2 from $C_T = 2 \times \sqrt{r^2 - (\overline{H} - r)^2} \times L$, where r and L is the radius and length of the tank, respectively.

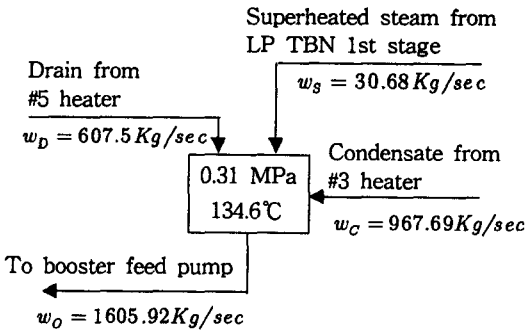

Fig. 7. Flow Rates at Steady State Power of 100%

With the sampling interval of 0.1*sec*, the system matrices of Eq.(6) are found to be

$$F = [0.9918],\ G = [3.931 \times 10^{-5}] \qquad (30)$$

The measurement matrix H and noise gain matrix T are regarded as unity. The process noise covariance and measurement noise covariance are assumed to be

$$\Gamma_w = 1 \times 10^{-2},\ \Gamma_v = 1 \times 10^{-2} \qquad (31)$$

Finally, the bias vector of

$$V^T = [-1.5,\ -1.0,\ 0,\ 1.0,\ 1.5] \qquad (32)$$

is applied as the sensor biases.

Corresponding to biases, five Kalman filters are constructed with the same initial weighting values of 0.2, and the elements of Markov transition matrix are determined as and θ_{ij} = (1 − 0.95)/(N − 1) and θ_{ii} = 0.95.

For the evaluation, two scenarios are considered.

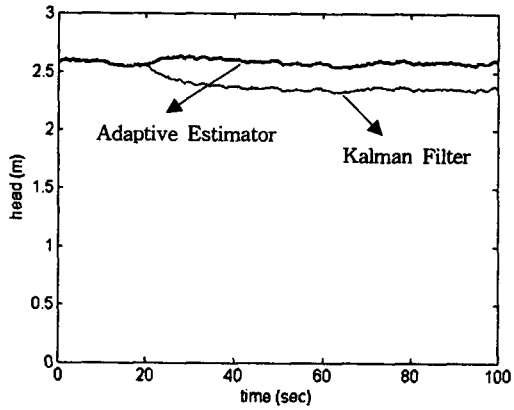

Fig. 8. Heads Estimated by Kalman Filter and Adaptive Estimator

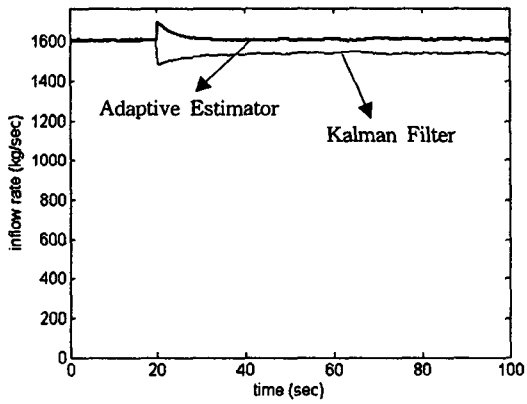

Fig. 9. Inlet Flow Rates by Kalman Filter and Adaptive Estimator

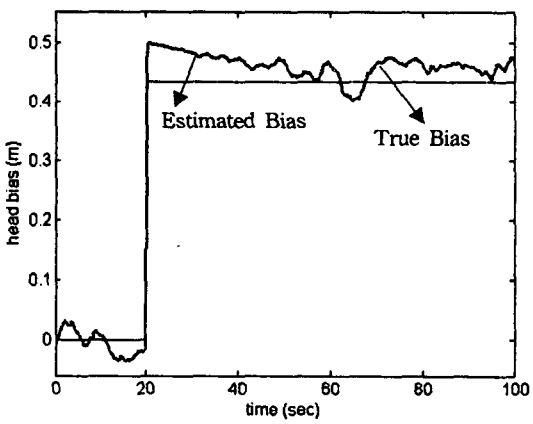

Fig. 10. True Bias and Estimated Bias

Scenario 1

In this scenario, it is assumed that the level sensor works normally during the first 20seconds, then is contaminated abruptly by a positive bias of v^b = 0.43m. Figure 8 shows the levels estimated by a classic Kalman filter and by the designed adaptive estimator.

During the sensor works normally, they are the same each other. But as the sensor fault occurs, the classic Kalman filter fails to estimate the actual level. On the other hand, the adaptive estimator calculates the bias of measurement sensor for the level compensation. By doing so, it is possible to maintain the constant level even in the case of sensor failure.

The corresponding inlet flow rates are compared each other in Fig. 9. With the occurrence of sensor failure, the Kalman filter decreases the inlet flow rate, while the adaptive controller makes the inlet flow rate constant except the short period of transient.

Figure 10 shows the ability of the bias estimation of the adaptive estimator. As shown in the figure, the adaptive estimator traces up the actual bias rather exactly.

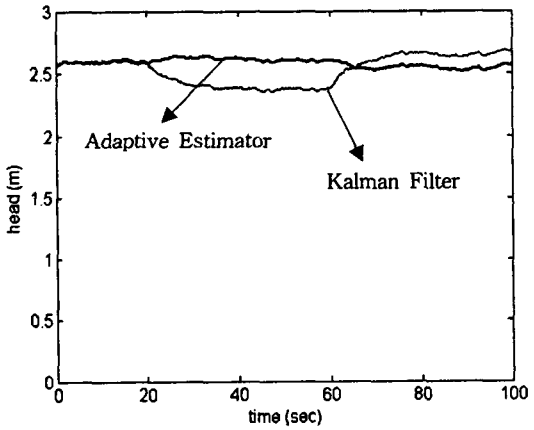

Fig. 11. Heads Estimated by Kalman Filter and Adaptive Estimator

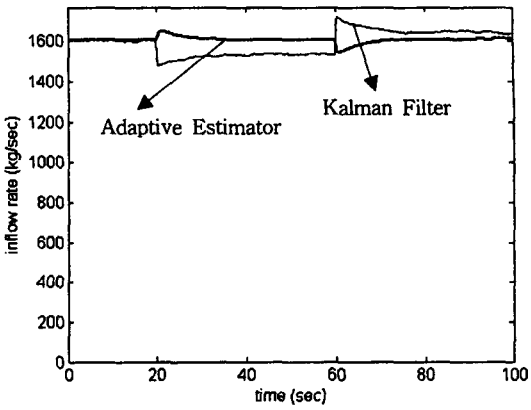

Fig. 12. Inlet Flow Rates by Kalman Filter and Adaptive Estimator

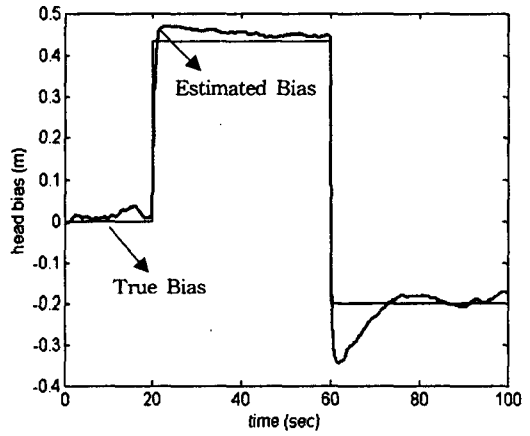

Fig. 13. True Bias and Estimated Bias

Scenario 2

This case is for the more fluctuating variation of sensor bias. The sensor is free of bias during the first 20 seconds. Then an abrupt positive bias of v^b = 0.43m is introduced to the sensor, and at t = 60sec, the bias changes to negative values of v^b = − 0.2m.

The levels controlled by the Kalman filter and by the adaptive estimator are described in Fig. 11, respectively. Similar to Fig. 8, both levels are the same during the first 20 seconds. But the level estimated by the Kalman filter is lower than the

normal level for the period of positive bias (t = 20 to t = 60), and becomes reverse with the introduction of negative bias. In contrast with the Kalman filter, the adaptive estimator makes the level almost constant, regardless of the bias. This indicates that the proposed estimator could maintain the same level even with the sensor failure.

The variations of inlet flow rate are shown in Fig. 12. With the Kalman filter, the flow rate becomes different with the value of bias. That is, the flow rate shows a decreased value during the positive bias acts on the sensor and increased one with a negative bias. Contrary to the Kalman filter, the flow rate controlled by the adaptive estimator is almost constant. With the introduction of bias, the flow rate shows a small transient, but recovers the normal value even with the biases.

Finally, Fig. 13 describes the bias calculated by the adaptive estimator and is similar to Fig. 10. It shows that the adaptive estimator can even trace up the wild change of bias. This indicates that the proposed estimator can identify the faults.

5. Conclusions

The software redundancy is no less important than the hardware redundancy with respect to the safety and reliability of the nuclear plants. In this paper, a software approach is made to increase the plant reliability by establishing an algorithm for the fault detection and diagnosis of the deaerator level sensor. With derivation of the deaerator model, the control model which consists of state equations and measurement equations is prepared. Then the control system in which an adaptive estimator detects the sensor faults are designed. By applying the proposed control system to the deaerator of Yonggwang 3 & 4, the performance of the designed system is verified.

References

1. R. Isermann, "Process fault detection based on modeling and estimation method-A survey," Automatica, vol.20, no.4, pp.387-404, (1984).
2. R. Isermann, et al., "Special section of papers on supervision, fault detection and diagnosis of technical systems," Control Engineering Practice, vol.5, no.5, pp. 637-719, (1997).
3. P.M. Frank, "Fault diagnosis in dynamic systems using analytical and knowledge based redundancy-A survey and some new esults," Automatica, vol.26, no.3, pp.459-474, (1990).
4. J. Gertler, "Survey of model-based failure detection and isolation in complex plants," IEEE Control Systems Magazine, vol.8, no.6, pp.3-11, (1988).
5. M. Basseville, "Detecting changes in signals and systems-A survey," Automatica, vol.24, no.3, pp.309-326, (1988).
6. R.W. Graingor, J. Holst, A.J. Isaksson, & B.M. Ninness, "A parametric statistical approach to FDI for the industrial actuator benchmark," Control Engineering Practice, vol.3, no.12, pp.1757-1762, (1995).
7. R.J. Patton, P.M. Frank, and R.N. Clark, Fault diagnosis in dynamic systems, theory and applications, Prentice-Hall, (1989).
8. A. Srinivasan and C. Batur, "Hopfield /ART-1 neural network-based fault detection and isolation", IEEE Trans. Neural Networks, vol.5, no.6, pp.890-899, (1994).
9. M.M. Polycarpou and A.T. Vemuri, "Learning methodology for failure detection and accommodation", IEEE Contr. Syst. Mag., pp.16-24, (1995).
10. P. Smyth, "Hidden markov models for fault detection in dynamic systems," Pattern Recognition, vol.27, no.1, pp.149 -164, (1994).

11. M. Kitamura, "Detection of sensor failures in nuclear plant using analytic redundancy," Transactions on American Nuclear Society, vol.34, pp.581-583, (1980).
12. K.A. Loparo, M.R. Buchner, and K.S. Vasudeva, "Leak Detection in an experimental heat exchanger process: A multiple model approach," IEEE Transactions on Automatic Control, vol.36, no.2, pp.167-177, (1991).
13. X.R. Li, and Y. Bar-Shalom, "Multiple-model estimation with variable structure," IEEE Transactions on Automatic Control, vol.41, no.4, pp. 478 - 493, (1996).
14. KHIC Process Specification - Deaerator, No. 028724-D01, Korea Heavy Ind. & Const.
15. K. Ogata, *System Dynamics*, Prentice Hall, (1998).
16. R.L. Moose, "Adaptive estimation for a system with unknown measurement bias", IEEE Transactions on aerospace and electronic systems, vol. AES-22, no.6, (1986).